Journal of Hazardous Materials 175 (2010) 423–428

Contents lists available at ScienceDirect

Journal of Hazardous Materials

journal homepage: www.elsevier.com/locate/jhazmat

Molecular dynamic simulations on the structures and properties of ε-CL-20(0 0 1)/F_{2314} PBX

Xiaojuan Xu[a,*], Jijun Xiao[b], Hui Huang[c], Jinshan Li[c], Heming Xiao[b]

[a] Department of Chemistry, Yancheng Teachers' College, Yancheng, 224002, PR China
[b] Institute for Computation in Molecular and Material Science and Department of Chemistry, Nanjing University of Science and Technology, Nanjing, 210094, PR China
[c] Institute of Chemical Materials, China Academy of Engineering Physics, Mianyang, 621900, PR China

ARTICLE INFO

Article history:
Received 22 July 2009
Received in revised form 6 October 2009
Accepted 6 October 2009
Available online 13 October 2009

Keywords:
Molecular dynamics (MD)
Polymer bonded explosives (PBX)
Mechanical properties
Pair correlation functions $g(r)$
Binding energies (E_{bind})
Detonation properties

ABSTRACT

Molecular dynamical (MD) simulations with the COMPASS force field were employed to investigate the influences of temperature (T), the concentration of F_{2314} binder (W%), and crystal defects on the mechanical properties, binding energy (E_{bind}), and detonation properties of ε-CL-20(0 0 1)/F_{2314} PBX (polymer bonded explosives). T was found to have some influences on the mechanical properties, and the PBX at 298 K was considered with better mechanical properties. By radial distribution function $g(r)$ analysis the three types of hydrogen bonds, H···O, H···F, and H···Cl were predicted as the main interaction formats between F_{2314} and ε-CL-20, and the strength of these interactions changed with temperature changing. The isotropic properties of the PBX increased with W% increasing, but each modulus and E_{bind} did not monotonously vary with W% increasing. The detonation properties of the PBX decreased with the increasing W%, and the PBX with 4.69% F_{2314} was regarded with good detonation properties. The existence of crystal defects (vacancy or adulteration) might increase the elasticity but destabilize the system to some extent, and the mechanical properties of PBX were chiefly determined by the main body explosive. The above information was thought guidable for practical formulation design of PBX.

1. Introduction

Polymer bonded explosives (PBX) are highly filled composite materials, comprising a high energy explosive material as the main body held together by a small amount of one or more kinds of polymeric binders. They are widely used in many defense and economic applications because PBX have many desirable traits such as good safety, high strength, ease of processing, etc. [1–3].

Hexanitrohexaazaisourzitane (CL-20) is a well-known high energy density compound (HEDC), and it has attracted much attention to find new CL-20-based PBX that show higher energy output, lower signature and decent sensitivity in explosive, propellant, and propelling agent formulations [4–19]. To our knowledge, however, there has been few theoretical studies on PBX to guide practice. In recent three or four years, our research group has put great effort into the investigations on the structures and performances of some PBX using molecular dynamics (MD) method [20–25]. As to ε-CL-20, MD simulations have been carried out to study the properties of 12 types of ε-CL-20-based PBX with four fluorine-polymers (PVDF, PCTFE, F2311, and F2314.) on the ε-CL-20 crystal surfaces (0 0 1), (0 1 0) and (1 0 0), respectively, and ε-CL-20(0 0 1)/F_{2314} PBX has been recommended as the energetic materials with better comprehensive performance [24]. Besides, the simulations on the ε-CL-20-based PBX with four different high energy oxidants (Estane5703, polyurethane; GAP, polyazideglyceraether, HTPB, hydroxy terminated, and PEG, polyethylene glycol) have successfully used to interpret the four main attributes (compatibility, mechanical properties, safety, and energetic properties) from experiments [25].

In practical formulation design of PBX, however, except to choose better binders to the main body explosive, many other factors affecting the properties of PBX should also be taken into account. For examples, the small adding of polymer binders can improve the mechanical properties but too high concentration of polymer binder will decrease the detonation properties of PBX; it will be bad for security when the temperature is too high; meanwhile, due to the influences of different growth conditions, such as light, impact, pressure, and radiation, it is difficult to obtain "perfect" crystals, but always those with some defects, such as vacancies and dislocations [26,27], many impurities, moreover, may be introduced during synthesis. All these so called crystal defects will destroy the integrality of crystal structures and affect the properties to different extent.

In this paper, therefore ε-CL-20(0 0 1)/F_{2314} PBX was further investigated as an NVT system to understand the influences of temperature (T), the concentration (W%) of F_{2314}, and different defects

* Corresponding author.
E-mail address: xxjn1@163.com (X. Xu).

0304-3894/$ – see front matter © 2009 Elsevier B.V. All rights reserved.
doi:10.1016/j.jhazmat.2009.10.023

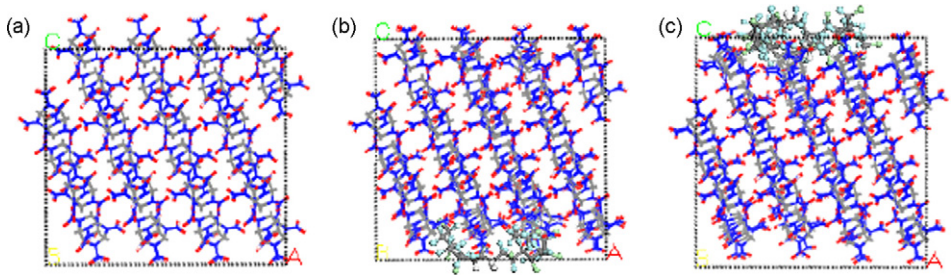

Fig. 1. Origin structures of (a) pure ε-CL-20, (b) ε-CL-20/F_{2314} with 4.69% of F_{2314}, and (c) with 9.45% of F_{2314}.

(mainly with vacancy and impurity) have on the mechanical properties and binding energies (E_{bind}), with the COMPASS force field [28] by MD simulations. These will not only add new basic data and rules of the structures and properties for ε-CL-20-based PBX, but also provide some instructive research methods and examples for the formulation of composite materials.

2. Computational methods

2.1. Modeling and simulation

The crystal parameters of ε-CL-20 were derived from X-ray diffraction [29]. The ε-CL-20 crystal was cut along the crystalline surface (0 0 1) with the "cutting" method in Material Studio (MS) 3.0.1 [30] and put in the periodic cells with 2.0 nm vacuum layer along the *z*-axis (*c* direction), and the periodic MD simulation cells contain 48 ε-CL-20 molecules, corresponding to $(2 \times 2 \times 3)$ unit cells. Fluorine resin F_{2314}, involving 10 chain segments was processed by amorphous cell module and simulated by 2.5 ns using the MD method to get the equilibrium conformations, and the end groups were saturated with F atoms. In constructing the original PBX models, different number (n = 0–5) of F_{2314} chains were put parallel to (0 0 1) surface of ε-CL-20, compressed and optimized by molecular mechanics (MM) adequately along the *c* direction until their densities (ρ = 2.055, 2.016, 2.039, 2.025, 2.012, and 2.001 g cm^{-3}, respectively) approach to the theoretical values, and the corresponding *W*% of F_{2314} reaches 4.69%, 9.45%, 12.86%, 16.44%, and 20.70%, respectively. In simulating the influences of *T*, the PBX with 9.45% F_{2314} (n = 2) was selected as the origin model, see as Fig. 1(b).

2.1.1. Defects with vacancies

To ensure the crystals with small proportion of vacancies, one ε-CL-20 molecule [(yellow colored as Fig. 2(a) and (b)] of the surface was removed, then the origin model of CRYSTAL2 and the corresponding PBX2 with 2% vacancies were built as Fig. 2.

2.1.2. Defects with adulteration

There always exists 2% or so 4,6,8,10,12-pentanitro-2-acetyl-2,4,6,8,10,12-hex-azaisowurtzitane (PNMAIW) in CL-20 prepared by the public nitrolysis methods [31–34], therefore the origin model of CRYSTAL3 and PBX3 were obtained when the ε-CL-20 molecule at the position of yellow sphere in Fig. 2(a) and (b) were substituted with a PNMAIW molecule, respectively, see Fig. 3(a) and (b).

The origin models above were considered as NVT ensembles and simulated by MD simulations using the COMPASS force field, which has been proved suitable for ε-CL-20 [24,25,35]. A fixed time step size of 1 fs was used in all cases. Equilibration runs of 200,000 fs were performed, followed by production runs of 120,000 fs, during which the data were collected for subsequent analysis.

2.2. Mechanical properties

The most general relation of a material between stress and strain obeys the generalized Hooke's law as the following:

$$\sigma_i = C_{ij}\varepsilon_j \tag{1}$$

where C_{ij} is (6×6) matrix of elastic coefficients. Due to existence of strain energy, the matrix is symmetric. Therefore, 21 coefficients are required to describe the relation between stress and strain for any material.

The stress tensors are obtained from the virial equation at atomistic level in static model as following [36]:

$$\sigma = -\frac{1}{V_0}\left(\sum_{i=1}^{N} m_i(v_i v_i^T)\right) \tag{2}$$

where m_i and v_i represent the atom mass and atom velocity, V_0 is the volume of system without deformation.

The stress imposed on a system will change the relative positions of particles of it. As for a parallel hexahedron (in simulation, the side lengths of the periodic box are *a*, *b*, and *c*, respectively), if row vectors a_0, b_0, and c_0 are the reference states, and vectors *a*, *b*, and *c* are deformation states, the strain tensors can be described as following:

$$\varepsilon = \frac{1}{2}[(h_0^T)^{-1} G h_0^{-1} - 1] \tag{3}$$

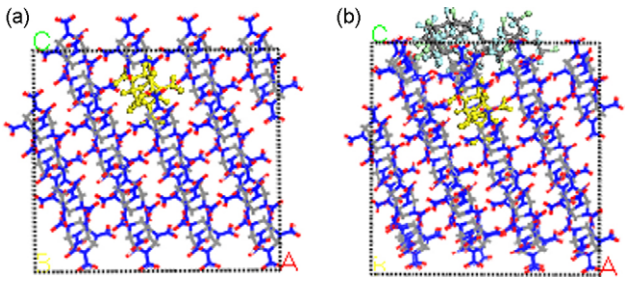

Fig. 2. Origin structures of (a) CRYSTAL2 and (b) PBX2 with 2.1% vacancies.

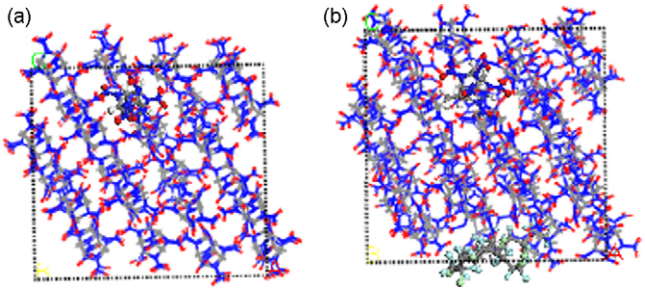

Fig. 3. Origin structures of (a) CRYSTAL3 and (b) PBX3 with 2.1% PNMAIW.

where h_0 is the matrix consisting of row vectors of a_0, b_0, and c_0; h is the matrix consisting of a, b, and c; G is the measurement tensor $h^T h$. By calculating the slope of tensile and shear deformations, the matrix of elastic coefficients can be obtained.

According to statistics, a heteromorphy consisting of microcrystals with random orientation can be considered isotropic. By Reuss mean method [37], its effective Bulk modulus and shear modulus can be calculated.

$$K_R = [3(a + 2b)]^{-1} \tag{4}$$

$$G_R = \frac{5}{(4a - 4b + 3c)} \tag{5}$$

where $a = 1/3(S_{11} + S_{22} + S_{33})$, $b = 1/3(S_{12} + S_{23} + S_{31})$, and $c = 1/3(S_{44} + S_{55} + S_{66})$. Coefficients matrix S of soft vectors is contrary to matrix C. Subscript R represents Reuss mean. As for most common crystal structures, 21 coefficients C_{ij} are independent, Reuss module only depends on nine soft vector coefficients. Based on the obtained K and G, tensile modulus (E) and Poisson's ratio (ν) can be calculated from the following:

$$E = 2G(1 + \nu) = 3K(1 - 2\nu) \tag{6}$$

2.3. Binding energy

Binding energy (E_{bind}) can accurately reflect the ability for the polymer binders to blend with the crystal and is defined as the negative value of interaction, that is, $E_{bind} = -E_{inter}$. Previous studies [25], furthermore, have shown that the PBX with larger E_{bind} will be more stable, and the compatibility is better. Thus E_{bind} is suggested to predict the compatibility of similar systems. As for a PBX in equilibrium, E_{bind} is calculated as the average of five frames in trajectory. The average E_{bind} between ε-CL-20 and polymer binder can be expressed as the following:

$$E_{bind} = -(E_T - E_{\varepsilon-CL-20} - E_{poly}) \tag{7}$$

where E_T is the average total energy of PBX, $E_{\varepsilon\text{-CL-20}}$ and E_{poly} are the average single point energies for ε-CL-20 and F_{2314} polymer, respectively.

2.4. Detonation properties

As an explosive, the heat of explosion (Q), detonation velocity (D), and detonation pressure (P) are important factors to evaluate its performance. The ω–Γ method [38] was chosen for our calculations because it is more suitable for both monomer and blending explosives. In this method, detonation velocity (D, m s^{-1}) is defined as the following:

$$D = 33.05Q^{1/2} + 243.2\omega\rho \tag{8}$$

where Q, ω, and ρ represent heat of explosion or the value of character heat (J g^{-1}), the factor of thermal energy, and the density of the loaded explosive (g cm^{-3}), respectively; as for the mixture explosives, the Q and ω are evaluated by adding Q_i and ω_i of each component according to their weight percent. Based on the simplification of the C–J (Chapman–Jouguet) theory of detonation wave [39] and D derived from Eq. (8), the detonation pressure (P, GPa) can be estimated by Eq. (9).

$$P = \frac{1}{4}\rho D^2 \times 10^{-6} \tag{9}$$

3. Results and discussion

3.1. Influences of temperature (T) on PBX

During MD simulations, it was found when $T = 448$ K, some ε-CL-20 molecules have deviated from their origin positions, thereby only ε-CL-20(0 0 1)/F_{2314} PBX in the temperature range of 248–398 K will be investigated.

Table 1
Effective elastic coefficients of ε-CL-20(0 0 1)/F_{2314} at different temperature.

T (K)	C_{11}	C_{22}	C_{33}	C_{44}	C_{55}	C_{66}	C_{12}	C_{13}	C_{23}	C_{12}–C_{44}
248	22.2	13.4	15.3	2.9	4.4	5.1	5.3	8.7	7.3	2.4
298	19.8	13.6	12.1	3.2	3.7	4.9	5.9	8.3	7.6	2.7
348	17.4	13.8	11.8	3.4	3.6	5.0	5.8	6.8	7.4	2.4
398	17.4	14.2	11.3	3.5	3.7	4.8	5.7	6.1	7.8	2.2

3.1.1. Mechanical properties

Due to that other elastic coefficients are approximate to zero, Table 1 only lists partial coefficients of ε-CL-20(0 0 1)/F_{2314} at different temperatures. From this table, most coefficients are found to decrease with T increasing, indicating that to produce the same strain anywhere, the stress needed to endure decrease, that is, the elasticity of the PBX increases as T increases. When these coefficients are divided into three groups (C_{11}, C_{22}, C_{33}; C_{44}, C_{55}, C_{66}; and C_{12}, C_{13}, C_{23}, respectively), the internal difference of each group is found to decrease, namely, the isotropicity of the PBX increases with the increasing temperature.

Besides, Cauchy pressure (C_{12}–C_{44}) can be used as a criterion to evaluate the ductibility and brittleness (the capability for deforming without cracking) of a material. Usually, the value of (C_{12}–C_{44}) for a ductile material is positive, contrarily, that is negative for a brittle material. According to this, it can be deduced from the positive values of (C_{12}–C_{44}) in Table 1 that in the temperature range of 248–398 K, ε-CL-20(0 0 1)/F_{2314} always takes on ductibility, and the PBX at 298 K is considered with better ductibility for its larger (C_{12}–C_{44}) value 2.7.

Tensile modulus (E), bulk modulus (K), and shear modulus (G) can be used to balance the ability for a material to resist elastic deformation. Meanwhile, the K value can also represent the rupture strength, that is, the greater the value of K is, the more energy will be required for a material to rupture. Tenacity is a property for a material to deform by absorbing energy, it can be predicted by the ratio (K/G) [40], and the greater K/G represents the better tenacity. Table 2 gives the values of E, K, G, and K/G for ε-CL-20(0 0 1)/F_{2314} at different temperature.

In Table 2 the Poisson's ratio values, ranging from 0.2 to 0.4, represent the plasticity of the PBX. With T increasing from 248 to 348 K, each modulus of E, K, and G decreases, predicting that the rigidity of the system decreases but elasticity increases; and it is the reason that with T increasing, the kinetic energy of the polymer molecules increases, the conformational change increases due to the internal rotation of one-axis, and the elasticity of the system increases accordingly, while $T = 398$ K, the little increase of E and G predicts the decreasing tendency of elasticity. Seen from the decreasing K, it is referred that the strength of rupture of the PBX monotonously decrease with increasing T. The larger K/G, together with the larger (C_{12}–C_{44}) in Table 1 show the better tenacity and ductibility of the PBX at 298 K.

3.1.2. Binding energy

From the values of E_{bind} in Table 3, it is obvious that with T increasing the total energy of the PBX (E_T), ε-CL-20 ($E_{\varepsilon\text{-CL-20}}$), and

Table 2
Mechanical properties of ε-CL-20(0 0 1)/F_{2314} at different temperatures.

T (K)	E (GPa)	G (GPa)	K (GPa)	ν	K/G
248	12.8	5.0	10.4	0.29	2.09
298	10.4	3.9	9.9	0.32	2.52
348	10.1	3.8	9.2	0.32	2.42
398	10.3	3.9	9.1	0.32	2.33

Table 3
Binding energies (E_{bind}) in ε-CL-20(0 0 1)/F_{2314} at different temperatures[a].

T (K)	E_T	$E_{\varepsilon\text{-CL-20}}$	$E_{F_{2314}}$	E_{bind}
248	−61968.17	−59981.16	−1219.85	767.16
298	−60758.56	−58882.32	−1128.22	748.01
348	−59712.35	−57842.25	−1128.81	741.28
398	−58518.66	−56737.90	−1025.98	754.78

[a] Unit: kJ mol^{-1}.

F_{2314} polymer chain ($E_{F_{2314}}$) increase due to the increase of molecular kinetic energies with increasing T; but there's a descending tendency to E_{bind} for that the fastly increasing kinetic energy will lead F_{2314} to depart from ε-CL-20, then the E_{bind} decreases.

It is also interesting to understand the interaction format. We will firstly introduce the concept of pair correlation function $g(r)$, also named radial distribution function. $g(r)$ gives a measure of the probability that, given the presence of an atom at the origin of an arbitrary reference frame, there will be an atom with its center located in a spherical shell of infinitesimal thickness at a distance r from the reference atom. This function has found applications in structural investigations of both solid and liquid packing (local structure), in studying specific interactions such as hydrogen bonding, in statistical mechanical theories of liquids and mixtures. And then three pairs of atomic interactions (H···O, H···F, and H···Cl) are considered. The H, F, and Cl atoms in F_{2314} are noted as H(1), F(1), and Cl(1), and the H and O atoms in ε-CL-20 molecules are named as H(2) and O(2), respectively. Because the distances between F_{2314} and inner ε-CL-20 are comparative far, so only the interactions between F_{2314} and ε-CL-20 molecules on the first two layers were investigated. Therefore, by employing the functions of $g(r)$ in MS 3.0.1 on the production trajectories, three types of $g(r)$ were obtained at different temperatures in Fig. 4.

Table 4
Mechanical properties of ε-CL-20(0 0 1)/F_{2314} with different W% of F_{2314}.

W%	Pure ε-CL-20	4.69%	9.45%	12.86%	16.44%	20.70%
C_{11}	27.0	20.8	19.8	19.0	18.1	15.5
C_{22}	18.1	11.3	13.6	13.6	13.1	11.3
C_{33}	15.1	12.0	12.1	11.4	10.4	9.3
C_{44}	3.8	3.2	3.2	2.4	2.8	2.7
C_{55}	7.6	2.8	3.8	3.7	3.6	2.5
C_{66}	8.1	3.5	4.9	4.5	3.7	2.2
C_{12}	3.1	4.8	5.9	5.2	4.1	4.4
C_{13}	8.0	7.9	8.3	6.7	5.7	5.0
C_{23}	5.0	6.7	7.6	5.6	4.7	5.1
$C_{12}-C_{44}$	−0.7	1.6	2.7	2.8	1.2	1.7
E (GPa)	17.8	10.7	10.4	11.4	11.4	9.4
K (GPa)	10.3	9.2	9.9	8.8	7.9	7.2
G (GPa)	7.4	4.1	3.9	4.4	4.5	3.7
ν	0.21	0.31	0.32	0.28	0.26	0.28
K/G	1.39	2.25	2.52	1.98	1.74	1.97

Generally, molecular interactions mainly include hydrogen bonds and vdW interactions, and the hydrogen bond is known as the main origin of molecular interaction. The distance range (r) for hydrogen bond is 2.0–3.1 Å, for strong vdW is 3.1–5.0 Å; and when r is farther than 5.0 Å, the vdW interaction is very weak. Several characteristics can be found from Fig. 4(a)–(d). Firstly, there always exists a strong peak in hydrogen bond region, indicating that the interactions are mainly the contribution of hydrogen bonds, together with certain vdW. Secondly, the contributions of different hydrogen bonds H(1)···O(2), F(1)···H(2), and Cl(1)···H(2) vary with temperature, namely, the probability $g(r)$ of the presence of the same atom pair is different at different temperature. Thirdly, hydrogen bonds are always dominant in the total interaction, thus the relative interaction strength can be deduced by comparing their peak values of $g(r)$. For example, from Fig. 4(a)–(d), it is found that the peak values of H(1)···O(2) [2.15] and F(1)···H(2)

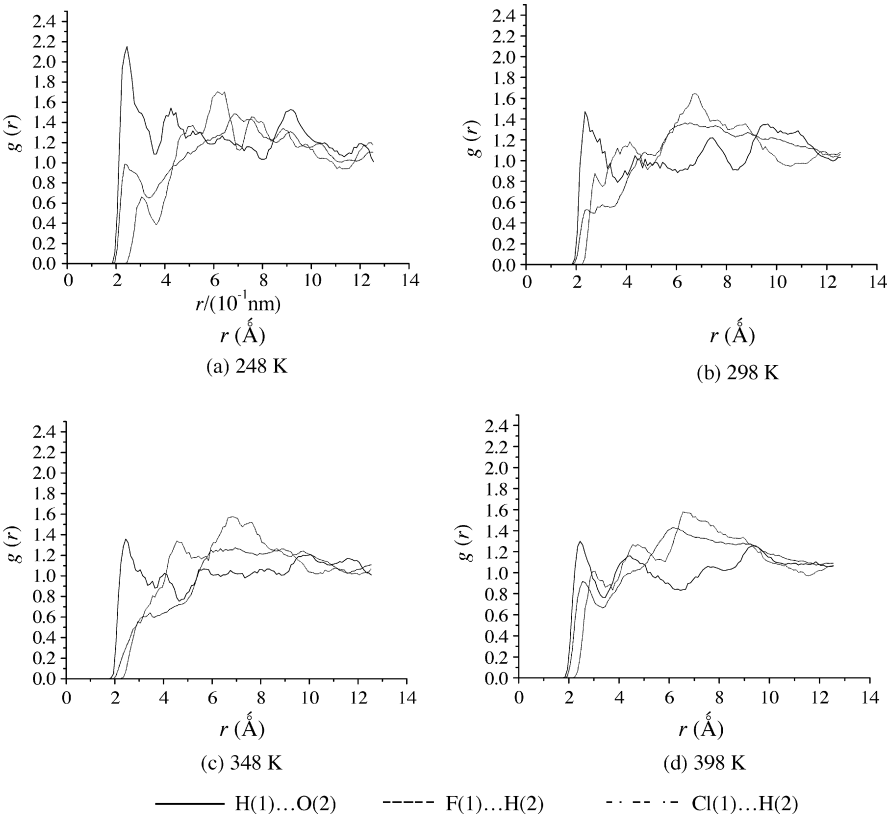

Fig. 4. Pair correlation functions $g(r)$ of the PBX at different temperatures.

Table 5
Binding energies (E_{bind}) and average binding energies (E_{aver}) in ε-CL-20(0 0 1)/F_{2314} with different W%[a].

n (W%)	E_T	$E_{\varepsilon\text{-CL-20}}$	$E_{F_{2314}}$	E_{bind}	E_{aver}
1 (4.69%)	−60016.82	−59034.27	−571.95	410.60	410.60
2 (9.45%)	−60758.56	−58882.32	−1128.22	748.01	374.03
3 (12.86%)	−61455.70	−58717.80	−1723.33	1014.70	338.08
4 (16.44%)	−62464.92	−58765.24	−2424.65	1275.03	318.77
5 (20.70%)	−63125.65	−58734.31	−3075.52	1315.82	263.17

[a] Unit: kJ mol^{-1}.

[0.98] in hydrogen region in Fig. 4(a) are the strongest, indicating that when T = 248 K, the total interactions are the strongest; as for Fig. 4(c), the peak value of H(1)···O(2) is only 1.36 or so, and mainly vdW interactions exists in F(1)···H(2) and Cl(1)···H(2), indicating the interactions between ε-CL-20 and F_{2314} are weaker when T = 348 K; while T = 398 K, the H(1)···O(2) interaction is weakened, but that of F(1)···H(2) and Cl(1)···H(2) is strengthened, and the total interaction is still stronger. Therefore the ordering of interactions between F_{2314} and ε-CL-20 in the PBX can be deduced as 248 K > 398 K > 298 K ≈ 348 K, this is consistent well with that from binding energies (E_{bind}) in Table 2, and the $g(r)$ can indeed be used to describe the interaction format.

3.2. Influences of the concentration (W%) of binder on PBX

3.2.1. Mechanical properties

Compared with the pure ε-CL-20, each elastic coefficient and modulus of PBX in Table 4 are found to decrease but the Cauchy pressure (C_{12}–C_{44}) and K/G to increase, predicting that the adding of polymer F_{2314} increases the elasticity, ductibility, and tenacity of the system. With the increasing of W%, the internal difference of each group (C_{11}, C_{22}, C_{33}; C_{44}, C_{55}, C_{66}; and C_{12}, C_{13}, C_{23}, respectively) decreases, and the isotropicity of the system increases. The Poisson's ratio of each PBX ranges from 0.26 to 0.32, little larger than that of pure ε-CL-20, showing the better plasticity of the PBX. Besides, it is also found that each physic parameter related to mechanical properties does not monotonously change with W%, that is, the PBX with larger W% does not mean its better mechanical properties, e.g., when W% increase from 4.69% to 9.45%, then to 12.86%, their tensile modulus (10.73, 10.42, and 1.35 GPa), bulk modulus (9.23, 9.90, and 8.76 GPa), and shear modulus (4.11, 3.93, and 4.42 GPa) are not proportional to W%. This will put forward more stringent requirements for PBX formulations.

3.2.2. Binding energy

Table 5 presents the total binding energy (E_{bind}) and the average binding energy ($E_{aver} = E_{bind}/n$, n = 1–5, the number of F_{2314} chains) between F_{2314} and ε-CL-20 molecules at 298 K. From Table 5, E_{bind} is found to increase with W% increasing, due to that it is a capacity property, not an intensity property; but the average binding energy (E_{aver}) decreases with increasing W%, and this can be explained that with W% increasing the F_{2314} polymer chains trend to glue to each other, an inherent characteristic of polymers, therefore the interaction between the two components of the PBX will weaken and E_{aver} decrease, namely, the additivity is not proper in calculating the E_{bind}.

3.2.3. Detonation properties

From Eqs. (8) and (9) it is found that detonation velocity (D) and detonation pressure (P) are mainly determined by the density (ρ), heat of explosion (Q) and the factor of thermal energy (ω) of explosives. Here, the theoretical density of F_{2314} is 2.02 g cm^{-3}, which is nearly equal to that of ε-CL-20 crystal (2.05 g cm^{-3}), therefore the W% of F_{2314} has little influence on the ρ of the ε-CL-20(0 0 1)/F_{2314} PBX; the Q and ω of F_{2314}, however, are much smaller than those of ε-CL-20 crystal, indicating that with W% increasing, the Q and ω of the PBX will decrease. Table 6 presents the calculated detonation parameters of the PBX with 0–20.7% of F_{2314}. From this table it can be seen that when W% > 4.69%, the related detonation parameters are comparative smaller and far away from the requirement of a good explosive. In all, when W% ≤ 4.69%, though the detonation properties of the PBX are poorer than those of the pure ε-CL-20, they are still satisfactory as high energy materials, and the concentration (W% = 4.69%) matches well with the practical formulation.

Table 6
Detonation properties of ε-CL-20(0 0 1)/F_{2314} with different W% of F_{2314}.

	0%	4.69%	9.45%	12.86%	16.44%	20.70%
Q (J g^{-1})	4623.8	4505.0	4384.4	4298.0	4207.3	4099.3
D (m s^{-1})	9025.1	8892.1	8653.3	8493.6	8333.5	8155.2
P (GPa)	40.8	39.9	38.2	36.5	34.9	33.3

3.3. Influences of crystal defects on PBX

3.3.1. Mechanical properties

Based on the production trajectories and static mechanical analysis, mechanical properties of three ε-CL-20 crystals ("perfect" CRYSTAL1, CRYSTAL2 with vacancies and CRYSTAL3 with adulteration) and their corresponding PBX with F_{2314} binder ("perfect" PBX1, PBX2 and PBX3) are obtained in Table 7.

Several characteristics can be drawn from the data in Table 7. Firstly, compared with the three crystals, the elastic coefficients and modulus of each corresponding PBX decrease but K/G increases to some extent due to the flexibility of polymer chain, namely, the adding of F_{2314} will decrease the rigidity but increase the elasticity and tenacity. Secondly, although the two above defects do not have obvious effects on the system, compared with the "perfect" CRYSTAL1, most modulus of CRYSTAL2 and CRYSTAL3 decrease, and therefore there is a tendency to increase their elasticity. Thirdly, few changes happen to the elastic coefficients and modulus of PBX2 and PBX3 compared with PBX1, though the change of PBX2 is larger, for instances, the tensile modulus (E), bulk modulus (K), and shear modulus(G) of PBX1, 10.7, 9.2 and 4.1 GPa are accordingly decreased to 9.3, 8.1, and 3.56 GPa of PBX2, viz., the vacancy defect may increase the elasticity of the system, this is in accord with the better elasticity of CRYSTAL2. That the values of K and K/G of PBX3 are larger, namely, PBX3 has better rupture strength and tenacity, also agrees well with the better corresponding performance of CRYSTAL3. According to these, it is inferred that the mechanical properties of PBX are chiefly determined by the main body explosive.

Table 7
Elastic coefficients, modulus, and densities (ρ) of three crystals and corresponding PBX.

	CRYSTAL1	PBX1	CRYSTAL2	PBX2	CRYSTAL3	PBX3
C_{11}	21.7	20.8	19.9	20.2	21.5	20.6
C_{22}	14.4	11.3	13.3	11.4	14.1	13.0
C_{33}	12.2	12.0	10.8	7.0	11.8	10.3
C_{44}	2.8	3.2	2.3	2.8	2.9	2.9
C_{55}	3.1	2.8	2.9	3.1	2.6	3.0
C_{66}	6.1	3.5	5.61	3.4	6.0	3.8
C_{12}	5.9	4.8	4.8	5.4	6.2	6.4
C_{13}	8.6	7.9	8.0	6.7	8.7	8.0
C_{23}	5.0	6.7	4.5	5.1	5.1	6.8
C_{12}–C_{44}	3.2	1.6	2.5	2.6	3.4	3.5
E (GPa)	12.2	10.7	11.4	9.3	11.8	10.0
K (GPa)	9.7	9.2	8.8	8.1	9.7	9.6
G (GPa)	4.7	4.1	4.5	3.6	4.8	3.8
ν	0.29	0.31	0.28	0.31	0.30	0.33
K/G	2.05	2.25	1.96	2.28	2.04	2.54
ρ (g cm^{-3})	2.055	2.039	2.012	2.016	2.055	2.016

Table 8
Binding energies (E_{bind}) between F_{2314} and ε-CL-20 molecules in three PBX[a].

PBX	PBX1	PBX2	PBX3
E_{bind}	410.60	370.25	375.94

[a] Unit: kJ mol^{-1}.

3.3.2. Binding energy

Table 8 gives binding energy (E_{bind}) of PBX1, PBX2, and PBX3 between ε-CL-20 and F_{2314} at 298 K. From this table the ordering of E_{bind} of three PBX is drawn as PBX1 > PBX3 > PBX2. This can be easily interpreted that the main interaction between F_{2314} and ε-CL-20 is hydrogen bond, the number of hydrogen bond is the most, and thus the interactions of PBX1 is the strongest; in PBX3 a CL-20 molecule is replaced by a PNMAIW, but the interaction between the later and F_{2314} is weaker; while in PBX2 one ε-CL-20 molecule is removed, the E_{bind} in PBX2 is the smallest, and this smallest E_{bind} presents that the vacancy defect may lower the stability of the system, and is not suitable for practical application.

4. Conclusions

Based on the MD simulation on the influences of temperature, the concentration (*W*%) of the F_{2314}, and ε-CL-20 crystal defects have on the ε-CL-20(0 0 1)/F_{2314} PBX, several illuminating information as following is obtained. Firstly, temperature has certain influences on the mechanical properties, such as elastic coefficients, modulus, ductibility, tenacity and so on, and the PBX at 298 K is considered with the better comprehensive properties. Three types of hydrogen bonds, H···O, H···F, and H···Cl are predicted as the main interactions between the F_{2314} and ε-CL-20 molecules by the analyses of pair correlation function $g(r)$, and the $g(r)$ curves can well describe the variations of the interactions with temperature increasing. Secondly, each physic parameter related to mechanical properties does not monotonously change with *W*%, and here the PBX with *W*% of 9.45% and 4.69% show preferable mechanical properties; total binding energy (E_{bind}) between the F_{2314} binder and ε-CL-20 molecules increases with *W*% increasing, but the binding energy of unit F_{2314} chain (E_{aver}) decreases with the increasing *W*%; with *W*% increasing, the detonation properties of the PBX decrease, the PBX with 4.69% F_{2314} is regarded with good detonation properties, and this content is much approximate to that in practical formulations(<5%); thirdly, crystal defect (with vacancy or adulteration) can improve the elasticity but destabilize the system due to the decreasing binding energy(E_{bind}); and the mechanical properties of PBX are chiefly determined by the main body explosive.

In all, temperature, the concentration of binder, and crystal defects always have influences on the properties (mechanical properties, binding energies and detonation properties) of crystals and corresponding PBX to some extent. Accordingly factors as many as possible should be taken into account in practical formulation design.

Acknowledgements

We gratefully thank the National Natural Science Foundation (20173028) and Natural Science Fund (08KJB4310016) for colleges and universities in Jiangsu Province, China.

References

[1] T.R. Gibbs, A. Popolato (Eds.), LASL Explosive Property Data, University of California Press, Berkeley, CA, 1980.
[2] H.S. Dong, F.F. Zhou, High Energy Explosives and Correlative Physical Properties, Science Press, Beijing, 1984.
[3] G.X. Sun, Polymer Blended Explosives, Defense Industry Press, Beijing, 1984.
[4] R.L. Simpson, P.A. Urtiew, D.L. Omellas, CL-20 performance exceeds that of HMX and its sensitivity is moderate, Propell. Explos. Pyrot. 22 (1997) 249–255.
[5] H.R. Bircher, P. Mäder, J. Mathieu, Properties of CL-20 based high explosives, in: 29th Int. Annu. Conf. ICT, Karlsruke, Germany, 1998, pp. 94–97.
[6] A. Donald, J. Geiss, Additional characterization of high performance CL-20 formulation, in: IM/EM Technology Symposium, NDIA, San Diego, 1999, pp. 129–140.
[7] J. Mathieu, CL-20 based formulations for shaped charge applications, in: IM/EM Technology Symposium, NDIA, San Diego, 1999, pp. 141–150.
[8] X.P. Pang, The application research of the performance of new explosive LX-19, Lett. Weapons 2 (2001) 6–11.
[9] P. Braithwaite, G. Dixon, M. Rose, R. Wardle, The promise of energetic TPE gun propellants-From notebook to full scale verification, in: 37th Annual Gun and Ammunition Symposium & Exhibition, NDIA, San Diego, 2002, pp. 15–18.
[10] L.Y. Chen, P.J. Yang, L.J. Zhang, S.Y. Heng, Study of the performance of explosive CL-20, Chin. J. Explos. Propell. 26 (2003) 65–67.
[11] U.R. Nair, R. Sivabalan, G.M. Gore, M. Geetha, S.N. Asthana, H. Singh, Hexanitrohexaazaisowurtzitane (CL-20) and CL-20-based formulations, Combust. Explos. Shock Waves 41 (2005) 121–132 (review).
[12] H.B. Song, Y.F. Liu, W.S. Yao, Properties of NEPE solid propellant containing hexanitrohexaazaisowurtzitane, Chin. J. Explos. Propell. 29 (2006) 44–46.
[13] L.Y. Chen, S.X. Zhao, P.J. Yang, S.Y. Heng, The coating and desensitization of CL-20, Chin. J. Energ. Mater. 14 (2006) 171–173.
[14] Y. Yang, Y.J. Luo, Y.B. Jiu, M.N. Du, Z. Ge, C.P. Cai, Influence of thermoplastic polyurethane elastomers (TPU) with different fraction of hard segments on the coating of CL-20, Chin. J. Energ. Mater. 15 (2007) 395–399.
[15] M.B. Talawar, R. Sivabalan, M. Anniyappan, G.M. Gore, S.N. Asthana, B.R. Gandhe, Emerging trends in advanced high energy materials, Combust. Explos. Shock Waves 43 (2007) 62–72.
[16] X. Wang, C.Z. Peng, Development of hexanitrohexaazaisowurtaitane at abroad, Chin. J. Explos. Propell. 30 (2007) 45–48.
[17] Y.X. Ou, Z. Meng, J.Q. Liu, Review of the development of application technologies of CL-20, Chem. Ind. Eng. Prog. 26 (2007) 1690–1694.
[18] Y. Yang, Y.J. Luo, Y.B. Jiu, M.N. Du, Y. Lv, Z. Ge, Influence of CL-20 coated with thermoplastic polyurethane elastomers (TPU) on mechanical properties of NEPE propellant, J. Solid Rocket Technol. 31 (2008) 358–363.
[19] H.Z. Hong, R. Xu, M. Huang, F.D. Nie, J.H. Zhou, Preparation and properties of reduced-sensitivity CL-20, Chin. J. Energ. Mater. 17 (2009) 125–126.
[20] J.J. Xiao, G.Y. Fang, G.F. Ji, H.M. Xiao, Simulation investigations in the binding energy and mechanical properties of HMX-based polymer-bonded explosives, Chin. Sci. Bull. 50 (2005) 21–26.
[21] J.J. Xiao, X.F. Ma, W. Zhu, Y.C. Huang, H.M. Xiao, A molecular dynamic simulation study of elastic properties of HMX-based and TATB-based PBXs, in: Proceedings of the eighth seminar "New trends in research of energetic materials", Pardubice, Czech Republic, 2005, pp. 19–21.
[22] Y.C. Huang, Y.J. Hu, J.J. Xiao, H.M. Xiao, Molecular dynamics simulation on the binding energy of TATB based PBX, Chin. J. Phys. Chem. 21 (2005) 425–429.
[23] J.J. Xiao, Y.C. Huang, Y.J. Hu, H.M. Xiao, Molecular dynamics simulation of mechanical properties of TATB/fluorine-polymer PBXs along different surfaces, Sci. Chin. Ser. B 48 (2005) 504–510.
[24] X.J. Xu, H.M. Xiao, J.J. Xiao, W. Zhu, H. Huang, J.S. Li, Molecular dynamics simulations for pure ε-CL-20 and ε-CL-20-based PBXs, J. Phys. Chem. B 110 (2006) 7203–7207.
[25] X.J. Xu, J.J. Xiao, H. Huang, J.S. Li, Molecular dynamics simulations on the structures and properties of ε-CL-20-based PBXs—primary theoretical studies on HEDM formulation design, Sci. Chin. Ser. B 50 (2007) 737–745.
[26] K. Huang, Physics of Solid, Advanced Educational Press, Beijing, 1988.
[27] J.Q. Chen, M.X. Chen, J.S. Zhao, Crystal Defects, Industry Press, Chekiang, 1992.
[28] H. Sun, An *ab initio* force-field optimized for condense-phase applications-overview with details on alkanes and benzene compounds, J. Chem. Phys. B 102 (1998) 7338–7364.
[29] X.Q. Zhao, N.C. Shi, Crystal structure of ε-hexanitrohexaazaisowurtzitane, Chin. Sci. Bull. 40 (1995) 2158–2160.
[30] Materials Studio 3.0, Accelys: San Diego, CA, 2004.
[31] A.T. Nielsen, Caged Polynitramine Compound, US 5,693,794 (1997).
[32] R.G. Duddu, P.R. Dave, Processes and compositions for nitration of N-substituted isowurtzitane compounds with concentrated nitric acid at elevated temperatures to form HNIW and recovery of gamma HNIW with high yields and purities, US 6,015,898 (2000).
[33] A.J. Sanderson, Process for making 2,4,6,8,10,12-hexanitro-2,4,6,8,10,12-hexaazatetracyclo [5.5.0.0.5,903,11]-dodecane, US 6,391,130, B1 (2002).
[34] V.L. Nikolaj, W. Ulf, G. Patrick, Synthesis and scale-up of HNIW from 2,6,8,12-tetraacetyl-4,10–dibenzyl-2,4,6,8,10,12-hexaazaisowurtzitane, Org. Proc. Res. Dev. 4 (2003) 156–158.
[35] X.J. Xu, W.H. Zhu, H.M. Xiao, Theoretical predictions on the structures and properties for polynitrohexaazaadaman-tanes (PNHAAs) as potential high energy density compounds (HEDCs), THEOCHEM 853 (2008) 1–6.
[36] R.J. Swenson, Comments-on-viral-theorems-for-bounded-systems, Am. J. Phys. 51 (1983) 940–942.
[37] J.P. Watt, G.F. Davies, R.J. O'Connell, The elastic properties of composite materials, Rev. Geophys. Space Phys. 14 (1976) 541–563.
[38] X. Wu, Simple method for calculating detonation parameters of explosives, J. Energ. Mater. 3 (1985) 263–277.
[39] L. Zhou, The Foundation of Explosive Chemistry, Beijing Institute of Technology, Beijing, 2005.
[40] S.F. Pugh, Relation between the elastic module and the plastic properties of polycrystalline pure metals, Philos. Mag. 45 (1954) 823–843.